Compatibility Conditions of Structural Mechanics for Finite Element Analysis

NASA Lewis Research Center, Cleveland, Ohio
and
R. H. Gallagher‡
Clarkson University, Potsdam, New York

The equilibrium equations and the compatibility conditions are fundamental to the analyses of structures. However, anyone who undertakes even a cursory generic study of the compatibility conditions can discover with little effort that, historically, this facet of structural mechanics has not been adequately researched by the profession. Now the compatibility conditions have been researched and understood to a great extent. For finite element discretizations, the compatibility conditions are banded and can be divided into three distinct categories: 1) the interface compatibility conditions, 2) the cluster, or field, compatibility conditions, and 3) the external compatibility conditions. The generation of the compatibility conditions requires the separating of a local region, next writing the deformation displacement relation for the region, and finally eliminating the displacements from those relations. The procedure to generate all three types of compatibility conditions is presented and illustrated through examples of finite element models. The uniqueness of the compatibility conditions thus generated is shown. The utilization of the compatibility conditions has resulted in the novel integrated force method. The solution that is obtained by the integrated force method converges with a significantly fewer number of elements, compared to the stiffness and the hybrid methods.

Nomenclature

n,m	= number of force and displacement variables
$r=(n\text{-}m)$	= number of compatibility conditions
$[B]$	= equilibrium matrix of dimension $(m \times n)$
$[C]$	= compatibility matrix of dimension $(r \times n)$
$[G]$	= flexibility matrix of dimension $(n \times n)$
$[K]$	= stiffness matrix of dimension $(m \times m)$
$[S]$	= governing IFM matrix of dimension $(n \times n)$
$\{\beta\}$	= deformation vector of dimension (n)

Introduction

In the analyses of structures both the conditions of equilibrium and of compatibility come into play, except for the trivial statically determinate case. The equilibrium equations, however, are more familiar to structural analysts than the conditions of compatibility, which were formulated only about a century ago.[1] The early forms of the compatibility conditions (CC), developed for the manual analyses of simple structures, were based on the concept of redundant structural elements. The notion of "cutting" the redundant members leading to the conditions of compatibility, formulated in the precomputer era, proved inconvenient and inefficient for large-scale automated computations, so they have almost disappeared from current practice. The general and mathematically rigorous CCs, analogous to St. Venant's strain formulation in elasticity,[1] have been formulated for finite element analysis. These conditions, referred to as the global compatibility conditions (GCC), are banded and are amenable to computer automation. The use of the CCs has resulted in the integrated force method.[2-16] In the integrated force method all the internal forces are treated as the primary unknown and the system equilibrium equations are coupled to the GCCs in a fashion paralleling approaches in continuum mechanics, such as the Beltrami-Michell formulation in elasticity.[17]

The CCs, in basic form, have been introduced and compared with the redundant CCs.[2-4] The purposes of this paper are 1) to describe the physical aspects of the CCs, including the interface CCs of finite element models; 2) to demonstrate the generation of the GCCs from their local counterparts; and 3) to illustrate the benefits that accrue from the use of the GCCs in finite element analysis. The subject matter of the paper is presented in the subsequent five sections. In the second section, the governing equations of the integrated force method (IFM) are presented. In the third section, the procedure to generate the CCs is given, and these concepts are illustrated in the fourth section. In the fifth section, comparison of results obtained by the IFM, the stiffness method, and the hybrid methods are presented, with the conclusions given in the sixth section.

Equations of the Integrated Force Method

In the integrated force method (IFM) of analysis, a discretized structure is designated as structure (n,m) where "structure" denotes the types of structure (truss, frame, plate, shell discretized by finite elements and their combinations, etc.), and (n,m) are force and displacement degrees of freedoms, respectively. The structure (n,m) has m equilibrium equations (EE) and $(r=n\text{-}m)$ CCs. The m EEs ($[B]\{F\}=\{P\}$) and the r CCs $[C][G]\{F\}=\{\delta R\}$ are coupled to obtain the governing equation:

$$\begin{bmatrix} [B] \\ \hline [C][G] \end{bmatrix} \{F\} = \begin{Bmatrix} P \\ \hline \delta R \end{Bmatrix} \quad \text{or } [S]\{F\}=\{P\}^* \tag{1}$$

where, $[B]$ is the $m \times n$ equilibrium matrix, $[C]$ is the $r \times n$

Received Nov. 20, 1989; revision received June 13, 1990; accepted for publication June 13, 1990.

*Senior NRC Fellow.
†Chief Scientist and Chief of Structural Mechanics. Member AIAA.
‡President. Fellow AIAA.

compatibility matrix, $[G]$ is the $n \times n$ concatenated flexibility matrix linking deformations $\{\beta\}$ to forces $\{F\}$ as $\{\beta\}=[G]\{F\}$, $\{P\}$ is the m component load vector, $\{\delta R\}$ is the r component effective initial deformation vector, $\{\delta R\} = -[C]\{\beta_0\}$; $\{\beta_0\}$ is the n component initial deformation vector, $[S]$ is the $(n \times n)$ governing matrix. The matrices $[B]$, $[C]$, $[G]$, and $[S]$ are banded and have full row ranks of (m, r, n, and n), respectively.

The solution of Eq. (1) yields the n forces $\{F\}$. The m displacements $\{X\}$ are obtained from the forces $\{F\}$ by back substitution:[9]

$$\{X\} = [J]\{[G]\{F\} + \{\beta_0\}\} \tag{2}$$

where, $[J]$ is the $m \times n$ deformation coefficient matrix defined as $[J] = m$ rows of $\{[S]^{-1}\}^T$

Equations (1) and (2) represent the two key relations of the integrated force method for finite element analysis to calculate forces and displacements, respectively.

Generation of the Compatibility Conditions

The compatibility conditions (CCs) and the associated coefficient matrix $[C]$ are obtained from St. Venant's strain formulation in elasticity, as an extension to discrete structural mechanics. The strain formulation is illustrated through the plane stress elasticity problem. The strain displacement relations of the problem are

$$\epsilon_x = \frac{\partial u}{\partial x}, \qquad \epsilon_y = \frac{\partial v}{\partial y}, \qquad \gamma_{xy} = \frac{\partial u}{\partial y} + \frac{\partial v}{\partial x} \tag{3a}$$

The CC is obtained by eliminating the two displacements from three strain displacement relations, as

$$\frac{\partial^2 \epsilon_x}{\partial y^2} + \frac{\partial^2 \epsilon_y}{\partial x^2} - \frac{\partial^2 \gamma_{xy}}{\partial x \partial y} = 0 \tag{3b}$$

The two steps necessary to generate the CCs are 1) establish the strain displacement relations given by Eq. (3a), and 2) eliminate displacements from the strain displacement relations to obtain the compatibility condition given by Eq. (3b).

In the mechanics of discrete structures, the deformation displacement relations are equivalent of the strain displacement relations in elasticity, deformations $\{\beta\}$ of discrete mechanics are analogous to strains $\{\epsilon\}$ in elasticity. The deformation displacement relations are obtained utilizing the relation between internal strain energy and external work, which for a discrete structure (n,m) can be written as

$$(1/2)\{F\}^T\{\beta\} = (1/2)\{X\}^T\{P\} \tag{4a}$$

Equation (4a) can be rewritten by eliminating loads $\{P\}$ in favor of internal forces $\{F\}$ using the EE $[B]\{F\} = \{P\}$ to obtain

$$(1/2)\{X\}^T[B]\{F\} = (1/2)\{F\}^T\{\beta\} \text{ or}$$

$$(1/2)\{F\}^T\{[B]^T\{X\} - \{\beta\}\} = 0 \tag{4b}$$

Since the force vector $\{F\}$ is not a null set, we obtain the following relation between member deformations and nodal displacements:

$$\{\beta\} = [B]^T\{X\} \tag{5}$$

Equation (5) represents the global deformation displacement relation of a finite element model whose system EEs are given as ($[B]\{F\} = \{P\}$). In Eq. 5, n deformations $\{\beta\}$ are expressed in terms of m displacements $\{X\}$; thus, there are ($r = n\text{-}m$) constraints on deformations, which represent the r CCs of the structure (n,m). The r CCs can be obtained by the elimination of the m displacements from the n deformation displacement relation. In matrix notation, the CCs can be written as

$$[C]\{\beta\} = \{0\} \tag{6a}$$

The CCs in terms of elastic deformations $\{\beta\}_e$ given by Eq. (6b) are obtained from Eq. (6a) and the definition of the total deformations $\{\beta\}$, initial deformations $\{\beta\}_0$ and elastic deformations $\{\beta\}_e$ as ($\{\beta\} = \{\beta\}_e + \{\beta\}_0$).

$$[C]\{\beta\}_e = \{\delta R\} \qquad \text{and} \qquad \{\delta R\} = -[C]\{\beta_0\} \tag{6b}$$

The matrix $[C]$ has dimension $r \times n$. It is rectangular and banded and it has full row rank r. The compatibility conditions are kinematic relationships, and these are independent of sizing design parameters (such as area of bars and moment of inertias of beams, etc.), material properties, and external loads. The compatibility conditions depend on the initial deformation in the structure. For numerical efficiency, direct elimination of displacements from the deformation displacement relation is not recommended for large scale computations. Instead, the global compatibility matrix $[C]$ is efficiently generated utilizing such physical features of finite element models as bandwidths and the determinacy of the grid points, etc.

Generation of the Global Compatibility Conditions

To generate the CCs:

1) Separate a local region from the structural model on the basis of interface, cluster, or external bandwidth considerations, as explained later in this section.

2) Establish the deformation displacement relations for the local region, and the elimination of the displacements yields the compatibility conditions for the region under consideration.

3) Repeat the first two steps until all ($r = n\text{-}m$) CCs of the structure (n,m) are generated.

These steps are elaborated in the fourth section. The order of generation of the CCs is immaterial; however, we recommend generating the interface conditions first since these are most numerous, followed by the cluster and finally the external CCs.

Bandwidths of the Compatibility Conditions

Based on bandwidth considerations, the CCs are divided into three distinct categories: interface, cluster or field, and external CCs. By assuming the example of a finite element model shown in Fig. 1, the three types of CCs are illustrated in Fig. 2.

Interface Compatibility Conditions

Numerous interfaces internal to the structure are created in the discretization processes. The interface is the common boundary shared by two or more elements. In Fig. 1, the common boundary along nodes 1 and 7 is the interface between elements 1 and 2, the boundary connecting nodes 12 and 17 is the interface between elements 13 and 14, and so on. The interface between elements 1 and 2 is shown in Fig. 2a. The deformations of elements 1 and 2 must be compatible along the common boundary defined by nodes 1 and 7, which gives rise to interface CCs. The number of CCs at the interface depends on the element types (such as membrane, flexure or solid tetrahedron, etc.) and their numbers. The maximum bandwidth of the interface CC (MBW_{icc}) can be calculated as

$$MBW_{icc} = \sum_{j=1}^{JT} (fof_{ej}) \tag{7a}$$

where MBW_{icc} represents the maximum bandwidth of the interface CCs; JT = total number of elements present at the interface; fof_{ej} represent the force degrees of freedom of the element j present at the interface.

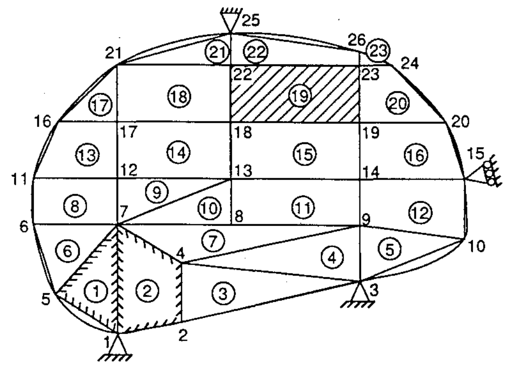

Fig. 1 Finite element model.

The bandwidth MBW_{icc} represents the maximum bandwidths of the interface CCs written either in terms of forces $\{F\}$ ($[C][G]\{F\} = \{0\}$), here we are referring to the bandwidth of the product matrix ($[C][G]$), or in terms of deformations $\{\beta\}$ as ($[C]\{\beta\} = \{0\}$), where the bandwidth is that of the compatibility matrix $[C]$. The interface CCs of discrete analysis are analogous to the boundary CCs in elasticity.[8] These are generated by writing the deformation displacement relation for the local interface (such as the interface defined by nodes 1 and 7 in Figs. 2a) and then eliminating the displacements. For the interface shown in Fig. 2a, there are two elements ($JT = 2$). Let us assume that both are membrane elements and that the force degrees of freedoms is 3 for the triangular and 5 for the quadrilateral elements. Then, the maximum bandwidth calculated from Eq. (7a) is $MBW_{icc} = 8$.

Cluster Compatibility Conditions

Consider any element in the model shown in Fig. 1, e.g., element 19. Element 19, along with its eight neighboring elements is also shown in Fig. 2b. The deformations of element 19 must be compatible with its neighboring elements (14–16 and 18–23). The CCs of the cluster of elements are referred to as the cluster CCs, which essentially represent St. Venant's strain formulation in the field. The maximum bandwidth of the cluster CCs can be calculated as

$$MBW_{ccc} = \sum_{j=1}^{JTC} (fof_{ej}) \tag{7b}$$

where MBW_{ccc} represents the maximum bandwidth of the cluster CCs, and JTC is equal to the total number of elements present in the cluster.

Assuming that the force degrees of freedom is 5 for quadrilateral and 3 for triangular elements, the bandwidth calculated from Eq. (7b) is $MBW_{ccc} = 41$. Generating the cluster CCs requires the establishment of the deformation displacement relation for the local clusters and then the elimination of the displacements.

External Compatibility Conditions

Reactions are induced at the restrained nodes. If such restraints on the boundary exceed the number of rigid body motions of the structure, then it is externally indeterminate. The degree of external indeterminacy of the structure can be calculated as

$$R_{\text{ext}} = N_x - N_f \tag{7c}$$

where R_{ext} is the number of external indeterminacy, N_x is the number of displacement components suppressed on the boundary, and N_f is the number of boundary conditions required only for the kinematic stability of the structure.

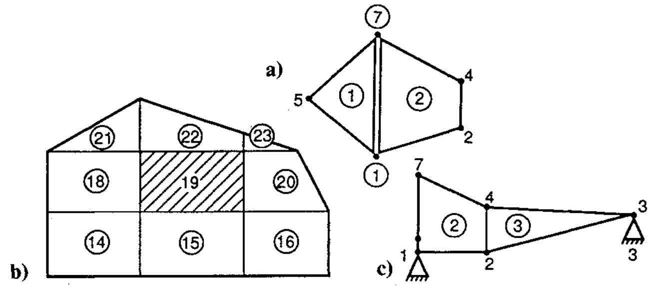

Fig. 2 Bandwidth of compatibility conditions; a) interface CC; b) cluster or field CCs; c) external CCs.

Let us assume the finite element model shown in Fig. 1 represents a membrane structure. Then its external indeterminacy is $R_{\text{ext}} = 7 - 3 = 4$, since the number of actual boundary restraints is $N_x = 7$, and the kinematic stability requirement is $N_f = 3$. To calculate the bandwidth of the external CCs, separate the local region connecting any two restrained boundary nodes. Let the number of elements between the nodes be represented by JTE, then the maximum bandwidth of the external CC MBW_{ccc} is given by

$$MBW_{ecc} = \sum_{j=1}^{JTE} (fof_{ej}) \tag{7d}$$

Assuming, as before, that force degrees of freedoms of quadrilateral and triangular elements are (5,3), respectively, then the maximum bandwidth of the external CC for the boundary segment shown in Fig. 2c is $MBW_{ecc} = 8$. The boundary CCs are obtained by the elimination of the displacements from the deformation displacement relations written for the local boundary segment.

The interface, cluster, and external CCs are the local constraints. The three categories of local conditions are concatenated together to form the system, or the GCCs of the structure (n, m). The sum of the number of interface (r_{icc}), cluster (r_{ccc}) and the external (r_{ecc}) CCs is equal to ($r = n\text{-}m$), of the structure (n, m) ($r = r_{icc} + r_{ccc} + r_{ecc}$).

Illustrative Examples

To illustrate the generation of the interface, cluster, external, and global CCs, we have selected a few simple finite element models that are idealized by triangular membrane and bar elements. The procedure, however, is general, and is applicable for different element types and discretizations. A computer code has been developed to generate GCCs for finite element models, and its element library includes bar, beam, quadrilateral and triangular membrane and plate flexure, solid brick and tetrahedron elements. The triangular and the bar elements are shown in Fig. 3. The membrane element has three force unknowns (F_{1e}, F_{2e}, and F_{3e}) and its six displacement degrees of freedom are ($X_{1e}, X_{2e}, \ldots, X_{6e}$). The bar element has one force and 4 displacement unknowns. For the membrane element, the (6×3) equilibrium matrix $[B]_e$ and (3×3) flexibility matrix $[G]_e$ are obtained in closed form[18]

$$[B]_e = \begin{bmatrix} -l_{12} & 0.0 & l_{31} \\ -m_{12} & 0.0 & m_{31} \\ l_{12} & -l_{23} & 0.0 \\ m_{12} & -m_{23} & 0.0 \\ 0.0 & l_{23} & -l_{31} \\ 0.0 & m_{23} & -m_{31} \end{bmatrix} \tag{8a}$$

$$[G]_e = \left(\frac{2}{Et}\right) \begin{bmatrix} \dfrac{\sin\theta_3}{\sin\theta_1 \sin\theta_2} & \cos\theta_2 \cot\theta_2 - \nu \sin\theta_2 & \cos\theta_1 \cot\theta_1 - \nu \sin\theta_1 \\ \cos\theta_2 \cot\theta_2 - \nu \sin\theta_2 & \dfrac{\sin\theta_1}{\sin\theta_2 \sin\theta_3} & \cos\theta_3 \cot\theta_3 - \nu \sin\theta_3 \\ \cos\theta_2 \cot\theta_2 - \nu \sin\theta_2 & \cos\theta_3 \cot\theta_3 - \nu \sin\theta_3 & \dfrac{\sin\theta_2}{\sin\theta_3 \sin\theta_1} \end{bmatrix} \tag{8b}$$

where l_{ij} and m_{ij} denote the direction cosines of the direction along the edge ij, E is the Young's modulus, ν is the Poisson's ratio, and t is the membrane thickness. The angles θ_i are defined in Fig. 3a.

Example I: The Membrane

Generation of the interface CCs is illustrated through the example of a membrane shown in Fig. 4a. The structure is made of steel, with Young's modulus $E = 30$ Ksi and Poisson's ratio $\nu = 0.3$, dimensions a and b are 100 in. and thickness $t = 1$ in. The loads are as depicted in Fig. 4a. The example is also solved herein by the integrated force method, and the stiffness solution in symbolic form is included for comparison. The membrane is idealized by two triangular elements. The discretization has six force degrees of freedom that are the concatenation of the two element force unknowns, such that

$$\{F\}^T = <F_1 = F_{1e1},\ F_2 = F_{2e1},\ \ldots,\ F_6 = F_{3e2}> \tag{9a}$$

where the subscript iej indicates the ith force of element j.

A corresponding deformation component (β_k) is associated with each force component (F_k). The six component deformation vector $\{\beta\}$ of the membrane is

$$\{\beta\}^T = <\beta_1 = \beta_{1e1},\ \beta_2 = \beta_{2e1},\ \ldots,\ \beta_6 = \beta_{3e2}> \tag{9b}$$

The five system displacement degrees of freedom shown in the Fig. 4a are represented by $\{X\}$ as

$$\{X\}^T = <X_1,\ X_2,\ \ldots,\ X_5> \tag{10}$$

The structure is designated as "membrane (6,5)" since it has 6 force and 5 displacement unknowns. The membrane (6,5) has 5 equilibrium equations and one ($r = 6\text{-}5 = 1$) compatibility condition.

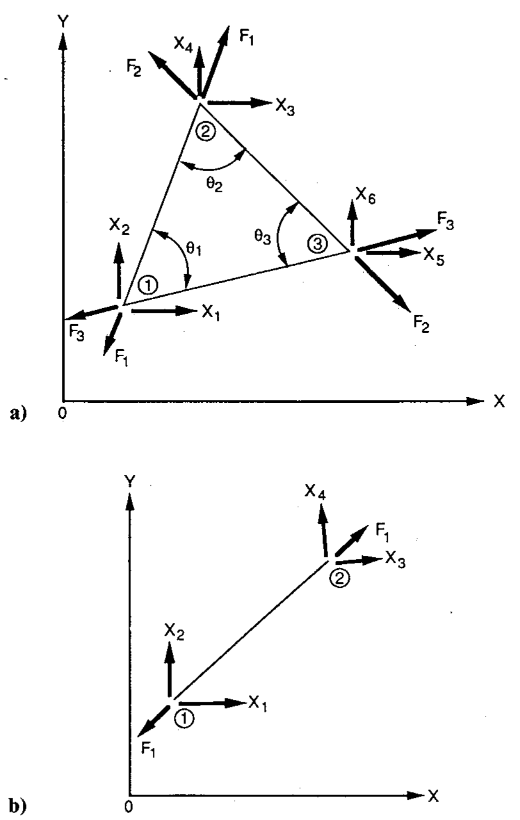

Fig. 3 Membrane and bar elements; a) membrane element; F_1, F_2, and F_3 are force degrees of freedom (*fof*) and X_1, X_2, ..., X_6 are displacement degrees of freedom; b) bar element; F_1 is the force degree of freedom and X_1, X_2, X_3, and X_4 are degrees of freedom.

Equilibrium Equations of the Membrane (6,5)

The five system EEs of the membrane (6,5) in terms of the six forces are obtained from the elemental equilibrium matrices following finite element assembly technique:

$$\begin{bmatrix} 1.0 & 0.0 & 0.7071 & 0.7071 & 0.0 & 0.0 \\ 0.0 & 0.0 & -0.7071 & -0.7071 & -1.0 & 0.0 \\ 0.0 & 1.0 & 0.7071 & 0.7071 & 0.0 & 0.0 \\ 0.0 & 0.0 & 0.0 & 0.0 & 1.0 & 0.0 \\ 0.0 & 0.0 & 0.0 & 0.0 & 0.0 & 1.0 \end{bmatrix} \begin{Bmatrix} F_1 \\ F_2 \\ F_3 \\ F_4 \\ F_5 \\ F_6 \end{Bmatrix} = \begin{Bmatrix} 50.00 \\ 100.00 \\ 50.00 \\ 50.00 \\ 100.00 \end{Bmatrix} \tag{11}$$

The five EEs cannot be solved for the six forces; one CC is required to augment Eq. (11) to a solvable set of 6 equations in 6 unknowns.

Compatibility Condition for the Membrane (6,5) or the Interface Compatibility Condition

Membrane (6,5) has one CC, therefore its local and global CC represent the same equation. The global deformation displacement relation (GDDR) of the membrane (6,5) required to generate its CC is obtained from Eqs. (5) and (11):

$$\begin{Bmatrix} \beta_1 \\ \beta_2 \\ \beta_3 \\ \beta_4 \\ \beta_5 \\ \beta_6 \end{Bmatrix} = \begin{bmatrix} 1.0 & 0.0 & 0.0 & 0.0 & 0.0 \\ 0.0 & 0.0 & 1.0 & 0.0 & 0.0 \\ 0.707 & -0.7071 & 0.7071 & 0.0 & 0.0 \\ 0.707 & -0.7071 & 0.7071 & 0.0 & 0.0 \\ 0.0 & -1.0 & 0.0 & 1.0 & 0.0 \\ 0.0 & 0.0 & 0.0 & 0.0 & 1.0 \end{bmatrix} \begin{Bmatrix} X_1 \\ X_2 \\ X_3 \\ X_4 \\ X_5 \end{Bmatrix} \tag{12}$$

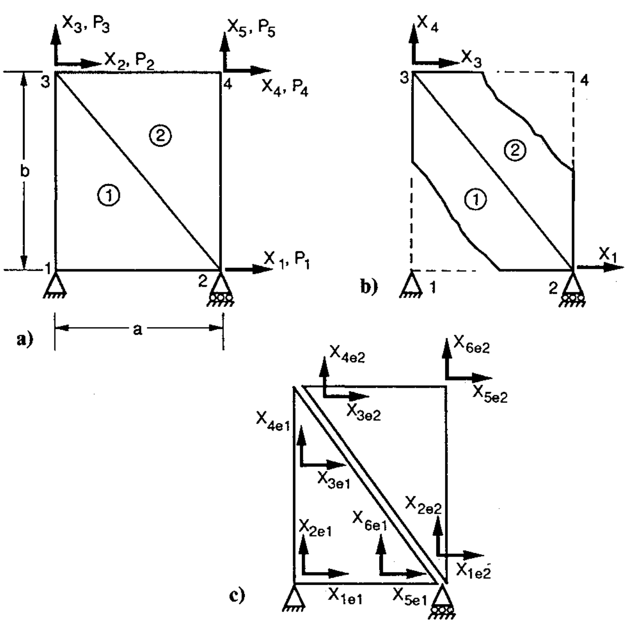

Fig. 4 Analysis of membrane; a) membrane; b) interface nodes 2 and 3; c) concatenated model.

The single compatibility condition for this problem can be obtained by the direct elimination of the five displacements from Eq. (12). The procedure is not recommended because it can become numerically expensive for large structures. The concept of node determinacy that enhances computational efficiency in the generation of the CC is presented next.

Node Determinacy Condition

The node determinacy for general application is presented first, then it is specialized for the membrane (6,5). The concept of determinate systems is extended to the nodes or grid points of a finite element model. Determinate nodes/grid points are identified and eliminated at intermediate stages of the generation of the CCs. Take any node of a finite element model, for example, the node i. Let K_i represent the number of force components present in the equilibrium equations written for that node i. Let L_i represent the displacement degrees of freedom of the node i, which is also equal to the number of equilibrium equations that can be written at that node. The indeterminacy of the node i designated NR_i is defined as

$$NR_i = K_i - L_i \tag{13}$$

If $NR_i = 0$, then the node i is designated determinate. Forces present at a determinate node i, referred to as determinate forces, do not participate in the CCs. Consequently, for determinate node i, K_i forces along with L_i equilibrium equations corresponding to $(L_i = K_i)$ displacements can be dropped simultaneously from the equilibrium matrix $[B]$ to obtain the reduced matrix $[B]^{(rl)}$ without affecting the CCs in any manner. Dropping forces and displacements is also equivalent to the elimination of appropriate columns and rows of the deformation displacement relations. The reduced deformation displacement relations (DDR_{rl}) obtained after imposing node determinacy condition, has the following form:

$$DDR_{rl} \quad \{\beta\}^{(rl)T} = [B]^{(rl)T}\{X\}^{(rl)} \tag{14}$$

In Eq. (14), the dimension of matrix $[B]^{(rl)T}$ is $\{(n - K_i)x\,(m - K_i)\}$, the deformation $\{\beta\}^{(rl)}$ and displacement $\{X\}^{(rl)}$ vectors have dimensions $n - K_i$ and $m - K_i$, respectively. The number of CC's contained in (DDR_{rl}) given by Eq. (14) is $r = \{(n - K_i) - (m - K_i)\}$ or $r = n\text{-}m$, since no CC has yet been generated. The node determinacy condition can reduce the number of deformation displacement relations from n to $n\text{-}K_i$; however, the number of CCs remain the same. The motivation behind dropping of determinate variables at the intermediate stage of the generation of the CCs is to enhance "Node Determinacy" at as many grid points as possible.

The membrane (6,5) has two determinate forces (F_5 and F_6) and these correspond to displacements (X_4 and X_5 at node 4) and equilibrium equations (4 and 5) in Eq. (11); therefore, $K_i = 2$ and $L_i = 2$. The node $i = 4$ is determinate, since $NR_i = K_i - L_i = 0$. The reduced deformation displacement relations obtained after incorporating the determinacy for node 4 has the following explicit form:

$$\begin{Bmatrix} \beta_1 \\ \beta_2 \\ \beta_3 \\ \beta_4 \end{Bmatrix} = \begin{bmatrix} 1.0 & 0.0 & 0.0 \\ 0.0 & 0.0 & 1.0 \\ 0.707 & 0.707 & 0.707 \\ 0.707 & 0.707 & 0.707 \end{bmatrix} \cdot \begin{Bmatrix} X_1 \\ X_2 \\ X_3 \end{Bmatrix} \tag{15}$$

The number of CCs given by Eq. (15) still remains one ($r = 4 - 3 = 1$), since no CC has yet been generated. The local structure that is obtained after the elimination of determinate node 4 is shown in Fig. 4b. Since node 1 is fixed and node 4 has been dropped, Eq. (15) represents the interface deformation displacement relation defined by nodes 2 and 3 and elements 1 and 2. The interface relation has four deformations (β_1, β_2, β_3, and β_4) expressed in terms of three displacements (X_1, X_2, and X_3). The elimination of the three displacements from Eq. (15) yield the single CC with the following explicit form:

$$(\beta_3 - \beta_4) = 0 \tag{16}$$

Equation (16) represents the deformation balance condition between adjoining elements 1 and 2 along the interface defined by nodes 2 and 3, and is referred to as the interface CC. For the membrane model, each interface has one interface CC. However, the number of CCs at an interface of any discrete model will depend on the type and number of elements connected to the interface. For example, the rectangular plate flexure element given in the fifth section has three CCs at each interface. The interface CCs represent the majority, though not all the CCs of a finite element idealization. The generation of the interface CC requires the establishment of the deformation displacement relation for the local interface, and then the elimination of the displacements.

The CC, $[[C]\{\beta\} = \{0\}]$ for the membrane (6,5) given by Eq. (16) has to be expressed in forces $[C][G]\{F\} = \{0\}$, so that it can be coupled to the equilibrium equations [Eq. (11)] to obtain the IFM governing equations $[[S]\{F\} = \{P\}^*]$. Transformation of deformations $\{\beta\}$ into forces $\{F\}$ is carried out by the constitutive relation $\{\beta\} = [G]\{F\}$. Here, the matrix $[G]$ of dimension (6×6) is the block diagonal concatenation of element matrices $\{[G]_e$ refer to Eq. (8b)$\}$ for elements 1 and 2. The interface CC, $(\beta_3 - \beta_4 = 0)$, in terms of forces, has the following form:

$$[0.5\ 0.5\ 1.0\ -1.0\ -0.5\ -0.5] \begin{Bmatrix} F_1 \\ F_2 \\ F_3 \\ F_4 \\ F_5 \\ F_6 \end{Bmatrix} = \{0\} \tag{17}$$

For the membrane (6,5), the maximum bandwidth of the CC is $MBW_{icc} = 6$, the actual bandwidth is $BW_{\text{actual }C} = 2$, and composite bandwidth is $BW_{\text{actual }CG} = 6$.

Solution of the Membrane (6,5) by the Integrated Force Method

For completeness, the solution of the membrane (6,5) by the IFM is presented. The equation $[S]\{F\} = \{P\}^*$ for the membrane (6,5) is obtained by coupling Eq. (11) to Eq. (17):

$$\begin{bmatrix} 1.0 & 0.0 & 0.7071 & 0.7071 & 0.0 & 0.0 \\ 0.0 & 0.0 & -0.7071 & -0.7071 & -1.0 & 0.0 \\ 0.0 & 1.0 & 0.7071 & 0.7071 & 0.0 & 0.0 \\ 0.0 & 0.0 & 0.0 & 0.0 & 1.0 & 0.0 \\ 0.0 & 0.0 & 0.0 & 0.0 & 0.0 & 1.0 \\ \hline 0.5 & 0.5 & 1.0 & -1.0 & -0.5 & -0.5 \end{bmatrix} \times \begin{Bmatrix} F_1 \\ F_2 \\ F_3 \\ F_4 \\ F_5 \\ F_6 \end{Bmatrix} = \begin{Bmatrix} 50.00 \\ 100.00 \\ 50.00 \\ 100.00 \\ 100.00 \\ \hline 0.0 \end{Bmatrix} \tag{18}$$

The solution to Eq. (18) yields the six forces; the displacements are obtained from forces by back substitution in Eq. (2). The forces and displacements are

$$\begin{Bmatrix} F_1 \\ F_2 \\ F_3 \\ F_4 \\ F_5 \\ F_6 \end{Bmatrix} = \begin{Bmatrix} 200.00 \\ 200.00 \\ -168.60 \\ -\ 43.58 \\ 50.00 \\ 100.00 \end{Bmatrix} \quad \begin{Bmatrix} X_1 \\ X_2 \\ X_3 \\ X_4 \\ X_5 \end{Bmatrix} = \begin{Bmatrix} 0.152 \\ -0.126 \\ 0.152 \\ 0.0260 \\ 0.152 \end{Bmatrix} \tag{19}$$

Analysis of the Membrane by the Stiffness Method

For comparison, the membrane is also analyzed by the stiffness method. The stiffness equations are well-known but complicated; therefore, the analysis is carried out in symbolic form. To establish the parallelism between the two methods, a slightly different procedure than normal is followed, the purpose will become evident in the process of solution. For the membrane, a displacement vector $\{X_c\}$of dimension 12, which represents the concatenation of the two elemental displacement degrees of freedom (see Fig. 4c), is defined as

$$\{X_c\}^T = \langle X_{c1} = X_{1e1},\ X_{c2} = X_{2e1},\ \ldots,\ X_{c12} = X_{6e2} \rangle \tag{20}$$

where the subscript (iej) represents the ith displacement component for the jth element.

Notice the similarities between the displacement vector $\{X_c\}$ of Eq. (20) and the force vector $\{F\}$ given by Eq. (9a). These represent the concatenation of the elemental displacements and forces, respectively. The equilibrium matrix in the stiffness method, in terms of concatenated displacement vector $\{X_c\}$, is obtained following assembly techniques as

$$[[K_1]\vdots[K_2]]\{X_c\} = \{P\} \tag{21}$$

The stiffness marix $[K_1]$ has dimension 3×6. Its three rows represent contributions to the equilibrium equations at node 2 along X_1, and at node 3 along X_2 and X_3 (see Fig. 4a), respectively. Likewise, the matrix $[K]_2$ has dimension 5×6, which contributes to the equilibrium at node 2 along X_1, node 3 along X_2 and X_3, and node 4 along X_4 and X_5. Equation (21) cannot be solved for the 12 displacements. Seven displacement CCs are required to augment Eq. (21) to a solvable 12×12 system. These are

$$X_{1e1} = 0, \qquad X_{2e1} = 0, \qquad X_{3e1} = X_{3e2}, \qquad X_{4e1} = X_{4e2},$$

$$X_{5e1} = X_{1e2}, \qquad X_{6e1} = 0, \qquad X_{2e2} = 0$$

The seven displacement continuity conditions can be represented by a single matrix equation:

$$[CTY]\{X_c\} = \{0\} \tag{22}$$

where the matrix $[CTY]$ is the displacement continuity matrix of dimension (7×12).

The five EEs [Eq. (21)] are coupled to the seven CCs [Eq. (22)] to obtain the (12×12) solvable equation system of the stiffness method:

$$\begin{bmatrix} [K_1\vdots K_2] \\ \hline [CTY] \end{bmatrix} \{X_c\} = \begin{Bmatrix} P \\ \hline 0.0 \end{Bmatrix} \tag{23}$$

Solution of Eq. (23) yields the displacements from which the internal forces can be recovered by back substitutions. From the equations of the integrated force [Eqs. (1) and (18)] and the stiffness [Eq. (23)] methods, we observe the following:

1) In the IFM, the EEs written in terms of forces are augmented by the CCs, also in forces.

2) In the stiffness method, the EEs expressed in terms of displacements are augmented by the displacement continuity conditions (CC).

3) The number of equations of the IFM [Eq. (18)] are fewer and sparser compared to stiffness equations [Eq. (23)]. (Details about equation sparsity and computations required by the methods are given in Ref. 14.)

4) The IFM satisfies both the equilibrium and the compatibility simultaneously, whereas the stiffness method is based on the eqilibrium and displacement continuity conditions.

Example II: Two-Bay Membrane

The generation of both interface and cluster CCs are illustrated using a two-bay membrane example, shown in Fig. 5. The structure is discretized by eight triangular elements and nine nodes. The discretization has 24 force and 15 displacement unknowns; it is designated membrane (24,15). It has 15 equilibrium equations and nine CCs. Because of increased complexity, the algebra for the example is presented in symbolic form. The system equilibrium matrix $[B_m]$ of dimension (15×24) is assembled following standard techniques. The global deformation displacement relations (GDDR) that correspond to the equilibrium matrix $[B_m]$ can be symbolized as

$$\text{GDDR: } \{\beta\} = [B_m]^T\{X\} \tag{24}$$

Equation 24 contains nine CCs since its 24 deformations are expressed in terms of 15 displacements. The membrane (24,15) shown in Fig. 5 has eight interfaces, along nodes 1–5 and nodes 5–8, etc. From example I, we know that each interface has one CC; therefore, the eight interfaces yield eight CCs, which can be generated following both parts of step I (Ia and Ib), explained as follows. Steps Ia, Ib, II, and III are parts of the general procedure to generate the CCs. For clarity, the steps are explained by using the example of membrane (24,15) as an illustration.

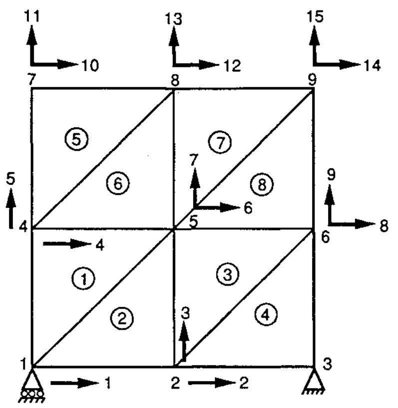

Fig. 5 Two-bay membrane.

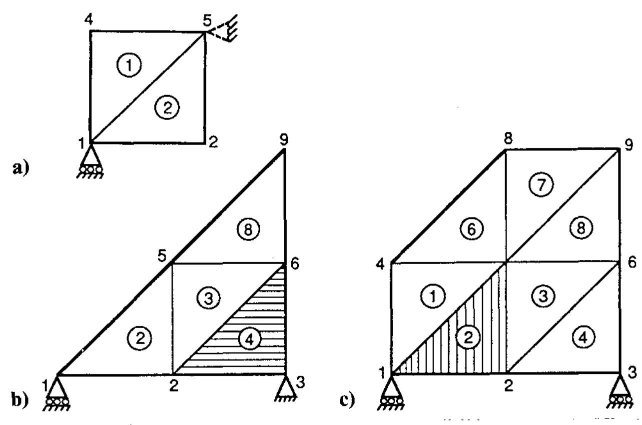

Fig. 6 Compatibility conditions for two-bay membrane; a) interface CC; b) determinate cluster; c) indeterminate cluster.

Step Ia: Local Structure and Interface Compatibility Condition

Consider any interface, for example, along nodes 1-5 between elements 1 and 2 for the membrane (24,15). Separate the interface and the elements, as shown in Fig. 6a. The local structure shown in Fig. 6a is statically unstable, therefore impose adequate numbers of restraints to ensure kinematic stability. Such restraints, which can be imposed at any of its nodes do not influence the CCs. The local structure requires two restraints, which are imposed at node 5. The stable local structure (6,5) has one interface CC. The local deformation displacement relation for the interface is extracted from the global deformation displacement relation. The interface deformation displacement relation consisting of six deformations (β_1, β_2, ..., β_6) expressed in terms of five displacements (X_1, X_4, X_5, X_6, and X_7) contains one CC that is generated following the procedure given for example I and it turns out to be $(\beta_3 - \beta_4) = 0$.

Step Ib: Update the Global Deformation Displacement Relations

The number of GDDRs of the structure (n,m) is reduced after the generation of each CC. The reduced set, designated ($GDDR_{r1}$), has $(m_1 = m)$ rows and $(n_1 = n - n_{c1})$ columns, where (n_{c1}) represents the number of CCs generated in step Ia. For the example, $n_{c1} = 1$, since only one CC was generated in step Ia. Its reduced deformation displacement relation ($GDDR_{r1}$) has 23 rows and 15 columns and contains eight CCs. It is obtained by dropping one deformation (β_3 or β_4) that has participated in the compatibility condition $(\beta_3 - \beta_4 = 0)$ generated in step Ia.

Step II: Local Structure and its Interface Compatibility Conditions

The local structure consisting of elements 2 and 3 is separated next, and its interface CC along nodes 2-6 are generated following steps Ia and Ib. Steps I and II are repeated until all the interface CCs have been generated. For this problem, there are eight interface CCs; at the end of their generation, the reduced deformation displacement relation ($GDDR_{r8}$) will have 16 rows and 15 columns containing one CC. Steps I and II are sufficient to generate all the interface CCs, which are the most numerous conditions in any finite element model. The computation required to generate the interface CCs is insignificant because only a few elements common to the interface participate in the generation process.

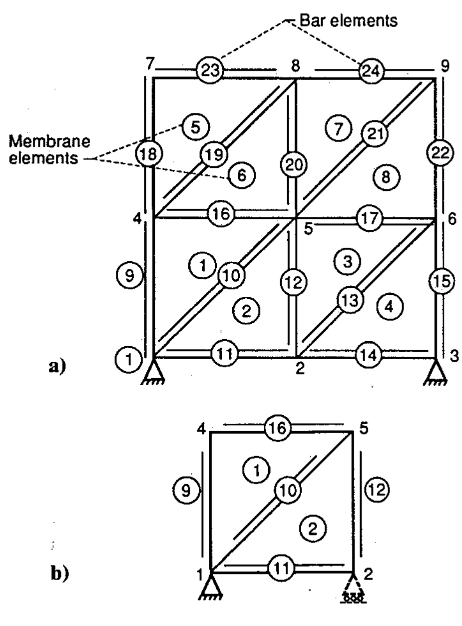

Fig. 7 Composite (membrane and bar) structure; a) model with eight membrane elements and 16 bar elements; b) interface CC.

Step III: Cluster Compatibility Conditions

In a finite element model, a cluster is defined as a series of adjoining elements. The cluster CCs represent constraints on the deformations of the elements that belong to the cluster. Take element 4 of the membrane (24,15). Its cluster, shown in Fig. 6b, consists of four elements (2, 3, 4, and 8) and six nodes (1, 2, 3, 5, 6, and 9). Let us designate its deformation displacement relation as ddr_{CL1}. The cluster is stable so there is no need to impose any restraints. The clusture is also determinate, since its nine deformations (β_4, β_6, β_9 to β_{12}, and β_{22} to β_{24}) (note β_5, β_7 and β_8 have been eliminated during the generation of the interface CCs) are expressed in terms of nine displacements (X_1 to X_3, X_6 to X_9 and X_{14}, X_{15}). The second cluster defined for element 2, shown in Fig. 6c, contains seven elements. Its deformation displacement relations (ddr_{CL2}) have 14 deformations (since seven deformations have been dropped during the generations of its seven interface CCs) expressed in terms of 13 displacements. The cluster contains one CC, which is obtained following steps Ia:

$$\{0.447(\beta_6 - \beta_2 + \beta_8 - \beta_{20}) - \beta_{16} - \beta_{12} + 0.894 \times (\beta_1 - \beta_5 + \beta_{17} - \beta_{23})\} = 0 \tag{25}$$

Step Ib is exercised, and the reduced $GDDR_{CL2}$ is obtained. Its 13 deformations are expressed in terms of 13 displacements. It contains no CC, thereby indicating that all nine conditions consisting of eight interface and one cluster CC have been generated for the membrane (24,15).

Example III: Stiffened Membrane

The generation of the external and interface CCs, when different element types are present in the discretization, is illustrated taking the example of the stiffened structure shown in Fig. 7. The structure is discretized by eight membrane and 16 bar elements. Nodes 1 and 3 of the model are fully restrained. The structure designated membrane (40,14) has $n = 40$ unknown forces consisting of the 24 membrane, 16 bar forces, and $m = 14$ displacement unknowns. Its $GDDR_{sm}$ contains 26 compatibility conditions, since its 40 deformations are expressed in terms of 14 displacements.

Interface Compatibility Conditions of Membrane (40,14)

The first interface defined by nodes 1-5 and associated membrane elements 1 and 2 and bars 9, 10, 11, 12, and 16 is considered. One boundary constraint, displacement at node 2, is imposed for its overall stability, as shown in Fig. 7b. This local structure has 11 force unknowns consisting of six membrane forces, five bar forces, and five unknown displacements, and it contains six compatibility conditions that are to be generated following step I. The six interface CCs are

$$(\beta_3 - \beta_4) = 0 \tag{26}$$

$$\beta_1 - \beta_9 = 0, \quad \beta_2 - \beta_{16} = 0, \quad \beta_3 - \beta_{10} = 0,$$
$$\beta_5 - \beta_{12} = 0, \quad \beta_6 - \beta_{11} = 0 \tag{27}$$

Equation 26 represents the membrane interface CC. The five bar-to-membrane interface conditions are given by Eq. (27). Steps I and II are repeated for the interfaces 4-5, 4-8, 5-8, 5-9, 5-6, 2-6, and 2-5, in turn to generate, respectively, (3, 3, 3, 3, 2, 3, 1) additional local interface CCs.

Cluster and External Compatibility Conditions of Membrane (40,14)

After the generation of the 24 interface CCs, the deformation displacement relation is reduced. Its 16 deformations are expressed in terms of 14 displacements, and it contains two compatibility conditions. Step III is evoked, yielding two CCs, one is a cluster CC [same as given by Eq. (25)]. The other, $(\beta_4 + \beta_{10} = 0)$, which represents a constraint on the deformations between the boundary nodes 1 to 3, is the external CC of the membrane.

External Compatibility Conditions of a Bridge Truss

A bridge truss supported at two nodes that are far apart, shown in Fig. 8a, further illustrates the generation of external CCs. The structure for analysis can be designated as truss (26,20); it has 20 EEs and six CCs. Its GDDR consists of 26 deformations that are expressed in terms of 20 displacements. The skeletal structures, such as trusses and frames, do not have any interface CCs; their CCs can be either cluster or external.

Cluster Compatibility Conditions of the Truss (26,20)

The cluster for element 1, consisting of six bars, is shown in Fig. 8b. The unstable cluster is made stable by imposing a constraint at node 3. The cluster designated as "bay (6,5)" has one CC that is obtained following Step I. At this time, any one bar (for example, bar 1) that corresponds to deformation β_1 is dropped; the determinate "bay (5,5)" obtained is shown in Fig. 8c. Steps I and II are repeated until all five cluster CCs are generated and the reduced structure shown in Fig. 8d is obtained.

External Compatibility Conditions

The reduced structure shown in Fig. 8d has one CC since its deformation displacement relation consists of 21 bar deformations expressed in terms of 20 displacements. The single CC is obtained by first imposing the node determinacy condition, which reduces the deformation displacement relation to six deformations expressed in terms of five displacements and then eliminating the displacements. The external CC ($\beta_2 + \beta_{10} + \beta_{15} + \beta_{20} + \beta_{25} = 0$) represents a homogeneous constraint on all the deformations between boundary nodes 1 and 12, as shown in Fig. 8e. The bandwidth of the external CC for restrained nodes that are far apart, typically encountered in long span bridges, can be large from physical considerations, since the deformations between fully constrained nodes of a truss far apart have to be zero

$$\sum_{i=1}^{5} \beta_{j(i)} = 0$$

The larger bandwidths of a few external CCs do not impose any major problem because in force method the solution process is carried out using sparse matrix techniques. Quite often such external CC's can be trivially generated by inspection.

Uniqueness of Compatibility Matrix

The CCs are homogeneous equations; therefore, these can be multiplied by any nonsingular matrix ($[R_u]$ for example) to obtain a feasible compatibility matrix $[C_u]$, given by Eq. (28). The feasible matrix $[C_u]$ is a linear combination of the rows of matrix $[C]$:

$$[R_u][C]\{\beta\} = \{0\} \qquad \text{or} \qquad [C_u]\{\beta\} = \{0\} \tag{28}$$

The procedure presented in this paper generates the matrix $[C]$ and not $[C_u]$. This is proved by observation. Take the example of two membrane interface CCs (CC_1 and CC_2) such that

$$CC_1\text{: } (\beta_{k1} - \beta_{k2} = 0) \qquad CC_2\text{: } (\beta_{k3} - \beta_{k4} = 0) \tag{29a}$$

A linear combination of CC_1 and CC_2 yields a feasible CC_3:

$$CC_3\text{: } \beta_{k1} - \beta_{k2} + \beta_{k3} - \beta_{k4} = 0 \tag{29b}$$

Notice that in CC_3, given by Eq. (29b), deformations present in CC_1, such as (β_{k1}, β_{k2}), and in CC_2 (β_{k3}, β_{k4}), are present. However, after the generation of CC_1, one of the two deformations (β_{k1} or β_{k2}) must be dropped (Step Ib); their combination cannot occur in subsequent CC's. In other words, after CC_1 has been generated, the feasible CC_3, which includes CC_1 cannot be obtained. Dropping a deformation that has participated in the CC immediately after its generation avoids the possibility of its further participation in any other CCs. The process generates the matrix $[C]$ and not its combinations, such as the usable matrix $[C_u]$. Therefore, the unique compatibility matrix $[C]$ is generated.

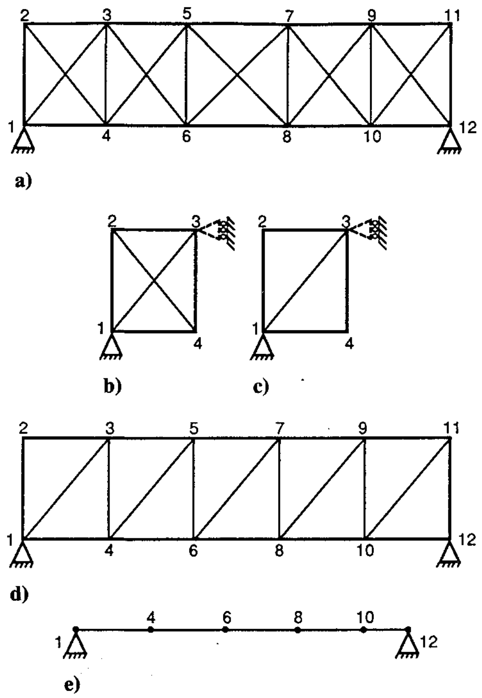

Fig. 8 Compatibility conditions of a bridge truss; a) bridge truss; b) indeterminate cluster; c) determinate cluster; d) reduced truss structure; e) external CCs.

Product of the Compatibility and Equilibrium Matrices is a Null Matrix

The product of the compatibility matrix $[C]$ and the equilibrium matrix $[B]$ is a null matrix ($[C][B]^T = [0]$). This can be verified by the substitution of the deformation displacement relation [Eq. (30b)] in the CC [Eq. (30a)]:

$$[C]\{\beta\} = \{0\} \tag{30a}$$

$$\{\beta\} = [B]^T\{X\} \tag{30b}$$

Eliminate deformations between Eqs. (30a) and (30b) to obtain

$$[C][B]^T\{X\} = \{0\} \tag{30c}$$

Since displacement $\{X\}$ is not a null vector, we obtain

$$[C][B]^T = [B][C]^T = [0] \tag{31}$$

The null product property of the two fundamental operators $[B]$ and $[C]$ implies that error in EEs can propagate to the CCs and vice versa.

Benefit Derived from the Compatibility Conditions

The accuracy of solutions obtained by the IFM or the stiffness or hybrid methods is of paramount importance, since all are approximate formulations. All methods attempt to satisfy the EEs written in terms of the forces or the displacements. However, explicit CCs, in a strict sense, are imposed only in the IFM. Any improved solution accuracy of the IFM over the other formulations should be a consequence of the explicit presence of the IFM's global CCs. Based on the theory of the IFM, a Generalized Integrated Force Technique (GIFT) computer code has been developed. To illustrate the solution accuracy in finite element calculations, a plate bending problem is solved by the GIFT code and other standard analyzers, such as MSC/NASTRAN,[19] ASKA[20] stiffness codes, a mixed formulation MHOST[21] and Chang's hybrid method.[22] The plate parameters considered are size of the plate (a = b = 40 in., 101.6 cm), aspect ratio a/b varied between 1 and 2, thickness of plate (h = 0.2 in., 5.08 mm), Young's modulus E = 30,000 ksi, 21,091.81 kg/mm²), and Poisson's ratio $\nu = 0.3$, the magnitude of concentrated load at the center (P = 500 lb, 226.795 kg). Both simply supported and clamped boundary conditions are considered. The central deflections of the plate, given by Timoshenko,[24] are $w_c = 0.2036$ in. (5.715 mm) for clamped case, and $w_c = 0.4217$ in. (11.712 mm) for simply supported boundaries.

To compare solution accuracy, the problem is solved using two types of elements: a four-node rectangular and a three-node triangular element. The IFM elements assume three forces (such as a shear force and two bending moments) and three displacements (transverse displacement and two slopes) per node. A cubic polynomial with 12 constants is used to approximate the transverse displacement in the element field. Normal moments M_x and M_y are assumed to have linear distributions and the twisting moment M_{xy} is constant in the element domain.[14]

The elements of the general purpose programs (NASTRAN, ASKA, and MHOST) are specialized to generate only the flexure solution. The elements used are 1) QUAD4 element—both ASKA and MSC/NASTRAN have QUAD4 elements, 2) TRIB3—triangular element of ASKA program, 3) TRIA3—triangular element of MSC/NASTRAN, and 4) TUBA3 of ASKA code. For bending response, the elements QUAD4, TRIB3, and TRIA3 represent three degrees of freedom per node. The TUBA3 of ASKA code is a higher order triangular element, with 6 degrees of freedoms per grid point. The hybrid elements have more unknowns, for flexural response. Chang's program has the equivalent of seven unknowns at the nodes, whereas mixed formulation MHOST has more unknowns per grid point. The IFM elements and the stiffness elements (such as QUAD4 of MSC/NASTRAN, QUAD4 of ASKA, TRIB3 of ASKA, and TRIA3 of MSC/NASTRAN) are equivalent with respect to their nodal degrees of freedom. The hybrid elements and TUBA-3 are higher order elements compared to IFM elements.

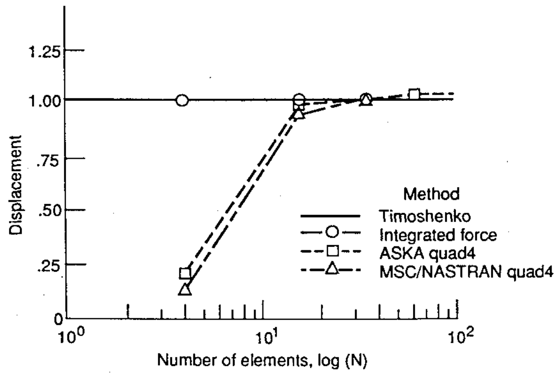

Fig. 9 Rate of convergence for rectangular elements.

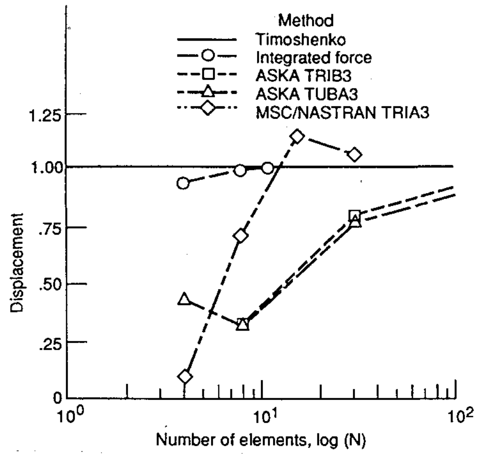

Fig. 10 Rate of convergence for triangular elements.

In the stiffness method, nodal stress parameters calculated from displacements by back substitution are discontinuous and ambiguous[23] at grid points, therefore calculation of forces at the nodes are routinely avoided. In this situation, the non-controversial nodal displacement is used in the comparison. Remember, however, that in IFM forces are the primary variables from which the secondary displacement unknowns are obtained by back substitution.

McNeal[25] has introduced a grading scheme for the evaluation of finite elements, as follows: A = less than 2% error, B = 2–10% error, C = 10–20% error, D = 20–50% error, and F = greater than 50% error. The results of the problems obtained by all four formulations are graded using McNeal's scheme and presented in Tables 1, 3, and 4. Results obtained by the IFM and the stiffness formulations are also presented graphically in Figs. 9 and 10. The IFM results for simply supported and clamped boundary conditions for different aspect ratios are presented in Table 2. From the numerical results of the plate flexure problem presented in Tables 1–4 and Figs. 9–10, we observe the following:

1) For the IFM rectangular element, convergence for the problem occurs for the first model, which has 4 elements. If symmetry is taken into consideration, then convergence occurs for a single element idealization. Both stiffness (MSC/NASTRAN and ASKA) and hybrid methods (MHOST and Chang's) converge slowly. To achieve grade A, MSC/NASTRAN QUAD4 element idealization requires 36 elements, whereas ASKA QUAD4 secures a B grade even for 100 elements. The hybrid method of Chang secures an A grade for 64 elements, whereas MHOST secures a B grade for the same level of discretization.

2) For the IFM triangular elements (see Fig. 10), the result is discernible from the analytical solution for the first model with four elements, but the result displays engineering accuracy. The next model, with eight elements, converges to the analytical solution and also achieves grade A. None of the stiffness elements, such as TRIA3 of MSC/NASTRAN and

Table 1 Rectangular element report card; clamped boundary condition

Number of elements for full plate	IFM	MSC/NASTRAN Quad 4	ASKA Quad 4
4 (2×2)	*A* (1.00)	*F* (0.13)	*F* (0.20)[a]
16 (4×4)	*A* (1.00)	*B* (0.94)	*B* (0.96)
36 (6×6)	*A* (1.00)	*A* (1.00)	*B* (1.03)
64 (8×8)	—	*A* (1.00)	*B* (1.03)
100 (10×10)	—	—	*B* (1.03)

[a]Unity (1.00) represents closed-form solution.

Table 2 Integrated Force Method; rectangular element report card

Number of elements for full plate	Aspect ratio	Clamped boundary	Simply supported boundary
4 (2×2)	1.00	*A*	*A*
16 (4×4)	1.00	*A*	*A*
4 (2×2)	1.20	*A*	—
4 (2×2)	1.40	*A*	—
4 (2×2)	1.60	*A*	—
4 (2×2)	1.80	*B*	—
4 (2×2)	2.00	*B*	—
8 (2×4)	2.00	*A*	—

Table 3 Rectangular element report card

Number of elements for full plate	IFM	Mixed method, MHOST	Hybrid method, Chang[22]
4 (2×2)	*A* (1.00)	*F* (0.06)	*F*
16 (4×4)	*A* (1.00)	*C* (0.85)	*C*
64 (8×8)	*A* (1.00)	*B* (1.13)	*A*

Table 4 Triangular element report card

Number of elements for full plate	IFM	MSC/NASTRAN TRIA 3	ASKA TRIB 3	ASKA TUBA 3
4	*B* (0.93)	*F*	—	*F* (0.42)
8	*A* (0.99)	*D*	*F* (0.31)	*F* (0.32)
16	*A* (0.99)	*C*	—	—
32		*B*	*C* (0.79)	*D* (0.76)
128			*B* (0.93)	*B* (0.90)

TRIB3 and TUBA3 of ASKA could secure grade A, even for models with fine discretization.

3) The IFM results for simply supported boundary follow the pattern of clamped boundary; namely, it secures grade A for the first model, which has four elements. The IFM element retains A grade for aspect ratio up to 1.6, and, for ratio 2.0, a total of eight elements, which correspond to a 2 × 4 mesh required for A grade. Other examples more or less follow the pattern depicted in Tables 1–4. Overall, the IFM convergence rate is very fast, whereas both stiffness and hybrid methods converge slowly or struggle to do so.

Conclusions

1) The structural mechanics profession recognizes that both equilibrium equations (EEs) and compatibility conditions (CCs) are essential for stress analysis. However, the CCs in typical finite element calculations were promoted via such concepts as "cuts" and closing the "gaps" or displacement matching (deflection or slope should have unique values), etc. Although such concepts are somewhat related to the CCs of finite element models, they do not represent the true CCs that are analogous to the strain formulation of St. Venant. The true CCs of finite element analysis have been understood to a great extent, though we do not claim that the understanding is total. Attempts should be made by the profession to understand the CCs in totality, rather than to avoid them because they are mathematically formidable or analytically more difficult than the familiar EEs.

2) In finite element analysis, the system EEs in terms of forces or displacements can be assembled from element matrices. The question is, can such an assembly technique be developed for the compatibility conditions also. The generation of the CCs is not exactly equivalent to the direct assembly technique of the finite element analysis, even though there is a close resemblance in that the global compatibility conditions are assembled from their local counterparts, such as interface, cluster, and external CCs. We do not as yet know a direct assembly scheme, but such possibility has not altogether been ruled out. We do, however, believe that the compatibility generation scheme given in this paper is rather elegant, since element characteristics and connectivities, etc., which are already contained in the EEs (and consequently in the deformation displacement relations) are referred to only once.

3) The compatibility conditions are unique. The computation time required to generate the compatibility condition is a small fraction of the total solution time.

4) Quality of solution in approximate methods is dependent on the extent to which equilibrium and compatibility conditions are satisfied. Since the integrated force method satisfies both the EEs and the CCs simultaneously, the solution via IFM is accurate, as expected. The stress parameters obtained by stiffness and hybrid methods do not satisfy even the EEs at the cardinal grid points; therefore, solution quality by such methods can be poor in comparison to IFM results.

5) Since all the finite element formulations are approximate in nature, we recommend generating solution via IFM and the stiffness method and comparing them, rather than qualifying the results obtained by any one formulation by successive mesh refinements.

References

[1]Love, A. E. H., *A Treatise on the Mathematical Theory of Elasticity,* 4th ed., Dover, NY, 1944.

[2]Patnaik, S. N., and Joseph, K. T., "Generation of the Compatibility Matrix in the Integrated Force Method," *Computer Methods in Applied Mechanics and Engineering,* Vol. 55, No. 3, 1986, pp. 239–257.

[3]Patnaik, S. N., and Joseph, K. T., "Compatibility Conditions from Deformation Displacement Relationship," *AIAA Journal,* Vol. 23, No. 8, 1985, pp. 1291–1293.

[4]Nagabhushanam, J., and Patnaik, S. N. "General Purpose Programme to Generate Compatibility Matrix in the Integrated Force Method," *AIAA Journal* (to be published).

[5]Patnaik, S., "An Integrated Force Method for Discrete Analysis," *International Journal for Numerical Methods in Engineering,* Vol. 6, No. 2, 1973, pp. 237–251.

[6]Patnaik, S. N., and Yadagiri, S., "Design for Frequency by the Integrated Force Method," *Computer Methods in Applied Mechanics and Engineering,* Vol. 16, No. 2, 1978, pp. 213–230.

[7]Patnaik, S. N., and Yadagiri, S., "Frequency Analysis of Structures by Integrated Force Method," *Journal of Sound and Vibration,* Vol. 83, No. 1, 1982, pp. 93–109.

[8]Patnaik, S. N., "The Variational Energy Formulation for the Integrated Force Method," *AIAA Journal,* Vol. 24, No. 1, 1986, pp. 129–137.

[9]Patnaik, S. N., "Integrated Force Method Versus the Standard Force Method," *Computers and Structures,* Vol. 22, No. 2, 1986, pp. 151–163.

[10]Patnaik, S. N., "Behaviour of Trusses with Stress and Displacement Constraints," *Computers and Structures,* Vol. 22, No. 4, 1986, pp. 619–623.

[11]Patnaik, S. N., and Gallagher, R. H., "Gradients of Behaviour Constraints and Reanalysis via the Integrated Force Method," *International Journal for Numerical Methods in Engineering,* Vol. 23, No. 12, 1986, pp. 2205–2212.

[12]Patnaik, S. N., and Naggraj, M. S., "Analysis of Continuum by the Integrated Force Method," *Computers and Structures,* Vol. 26, No. 6, 1987, pp. 889–905.

[13]Vijayakumar, K., Krishna Murty, A. V., and Patnaik, S. N., "A Basis for the Analysis of Solid Continua Using the Integrated Force Method," *AIAA Journal,* Vol. 26, No. 5, 1988, pp. 628–629.

[14]Patnaik, S. N., Berke, L., and Gallagher, R. H., "Integrated Force Method Versus Displacement Method for Finite Element Analysis," NASA TP-2937, Feb. 1990.

[15]Patnaik, S. N., "Analytical Initial Design for Structural Optimization via the Integrated Force Method," *Computers and Structures,* Vol. 33, No. 1, 1989, pp. 265–268.

[16]Patnaik, S. N., and Satish, H. G., "Analysis of Continuum Using Boundary Compatibility Conditions of Integrated Force Method," *Computers and Structures,* Vol. 34, No. 2, 1990, pp. 287–295.

[17]Sokolnikoff, I. S., *Mathematical Theory of Elasticity,* 2nd ed., McGraw-Hill, NY, 1956.

[18]Przemieniecki, J. S., *Theory of Matrix Structural Analysis,* McGraw-Hill, NY, 1968.

[19]Joseph, J. A., ed., MSC/NASTRAN, The MacNeal-Schwendler Corp., Los Angeles, CA, 1981.

[20]Argyris, J. H., "ASKA—Automatic System for Kinematic Analysis," *Nuclear Engineering and Design,* Vol. 10, No. 4, 1969, pp. 441–455.

[21]Nakazawa, S., "MHOST Version 4.2, Vol. 1: Users' Manual, "MARC Analysis Research Corp., Palo Alto, CA, NASA CR-182235-VOL-1, 1989.

[22]Saleeb, A. F., and Chang, Y. T., "An Efficient Quadrilateral Element for Plate Bending Analysis," *International Journal for Numerical Methods in Engineering,* Vol. 24, No. 6, 1987, pp. 1123–1155.

[23]Joseph, J. A., ed., "Stress Recovery at Grid Points," *MSC/NASTRAN Application Manual,* Sec. 2.2, McNeal-Schwendler Corp., Los Angeles, CA, 1982.

[24]Timoshenko, S., *Theory of Plates and Shells,* 2nd ed., McGraw-Hill, NY, 1959.

[25]MacNeal, R. H., and Harder, R. L., "A Proposed Set of Problems to Test Finite Element Accuracy," *Finite Elements in Analysis and Design,* Vol. 1, No. 1, 1985, pp. 3–20.